Journal of the Korean Magnetic Resonance Society **2015**, *19*, 99-105
DOI 10.6564/JKMRS.2015.19.3.099

Oxidation-induced conformational change of Hsp33, monitored by NMR

Yoo-Sup Lee[1,2†], Ji-Hoon Kim[1†], Min-Duk Seo[2,3], Kyoung-Seok Ryu[4], Eun-Hee Kim[4], and Hyung-Sik Won[1,*]

[1]Department of Biotechnology, College of Biomedical and Health Science, Konkuk University, Chungju, Chungbuk 27478, Korea
[2]Department of Molecular Science and Technology, Ajou University, Suwon, Gyeonggi 16499, Korea
[3]College of Pharmacy, Ajou University, Suwon, Gyeonggi 16499, Korea
[4]Protein Structure Group, Korea Basic Science Institute, Ochang, Chungbuk 28119, Korea

Received Sep 12, 2015; Revised Oct 27, 2015; Accepted Nov 25, 2015

Abstract Hsp33 is a prokaryotic molecular chaperon that exerts a holdase activity upon response to an oxidative stress at raised temperature. In particular, intramolecular disulfide bond formation between the four conserved cysteines that bind a zinc ion in reduced state is known to be critically associated with the redox sensing. Here we report the backbone NMR assignment results of the half-oxidized Hsp33, where only two of the four cysteines form an intramolecular disulfide bond. Almost all of the resolved peaks could be unambiguously assigned, although the total assignments extent reached just about 50%. Majority of the missing assignments could be attributed to a significant spectral collapse, largely due to the oxidation-induced unfolding of the C-terminal redox-switch domain. These results support two previous suggestions: conformational change in the first oxidation step is localized mainly in the C-terminal zinc-binding domain, and the half-oxidized form would be still inactive. However, some additional regions appeared to be potentially changed from the reduced state, which suggest that the half-oxidized conformation would be an intermediate state that is more labile to heat and/or further oxidation.

Keywords Hsp33, molecular chaperone, oxidative stress, backbone NMR assignments, conformational change

Introduction

A prokaryotic molecular chaperone, Hsp33, protects cells from extreme oxidative stress, by exerting a holdase activity that prevents irreversible denaturation of unfolding clients.[1,2] The post-translational activation of Hsp33 depends on the cellular redox potential, while its expression is increased by heat stress at transcriptional level. Generally, Hsp33 requires both the heat and oxidative stressors for its functional activation. However, alternatively, the protein was reported to be activated by HOCl, a major component of bleach, without elevating temperature.[3]

Hsp33 can adopt several different conformations according to the redox status and functional situation: the reduced monomer, reduced dimer, half-oxidized monomer, oxidized monomer, oxidized dimer, and oxidized oligomer forms. In particular, the oxidation-induced activation process of Hsp33 is

† These authors contributed equally to this work.

* Address correspondence to: **Hyung-Sik Won,** Department of Biotechnology, College of Biomedical and Health S cience, Konkuk University, Chungju, Chungbuk 27478, Korea, Tel: 82-43-840-3589; Fax: 82-43-852-3616; E-mail: wonhs@kku.ac.kr

triggered by intramolecular disulfide bond formation of the four conserved cysteines that bind a zinc ion in their reduced state. Oxidation of the cysteines leads to the release of zinc ion and subsequent unfolding of the C-terminal redox-switch domain. Finally, Hsp33 is activated by exposing hydrophobic surfaces that can bind folding intermediates as substrates.

Although several crystal structures of Hsp33 are available from different species, a controversy exists over their physiological relevance and functional status.[4] In particular, it is not clear whether the conformation at the half-oxidized state, where only two of the four conserved cysteines form a disulfide bond, is functionally active or not. Recently, we could generate a highly reliable, semi-empirical structure of the *Escherichia coli* Hsp33 in reduced state, by NMR spectroscopy in solution. In the present study, in order to investigate the oxidized conformations, we approached first the half-oxidized form, by NMR in solution.

Experimental Methods

Protein preparation - The expression plasmid pUJ30 encoding Hsp33 was transformed into *E. coli* BL21(DE3)pLysS[1,4]. Isotope-enriched NMR sample was prepared as described previously.[6] In order to produce the isotope-[^{13}C, ^{15}N]-enriched protein, the transformed cells were grown at 37°C in M9 minimal

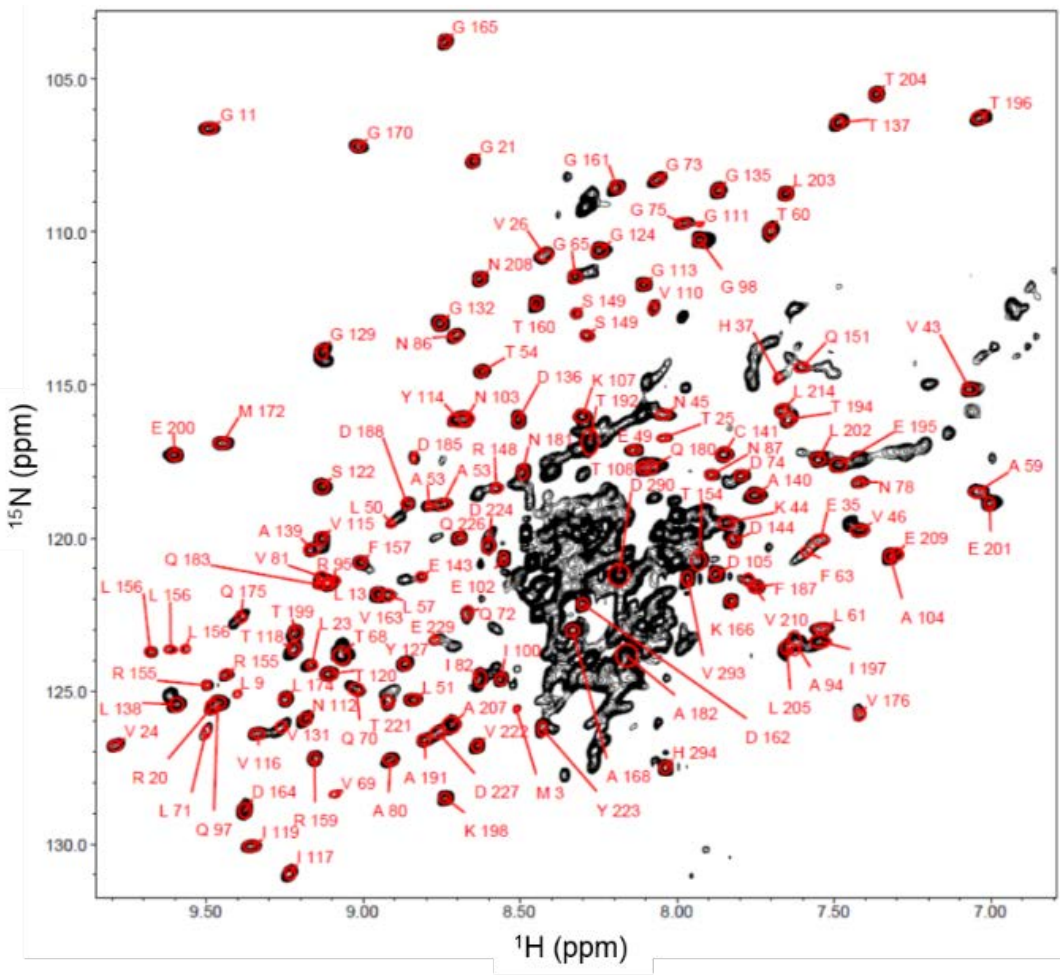

Figure 1. 2D-[^{1}H, ^{15}N]TROSY spectrum of the half-oxidized Hsp33. Sequence specific assignments are labeled in red on corresponding peaks in the spectrum.

medium, which was supplemented with [^{15}N]NH_4Cl and [^{13}C]glucose, as the sole source of nitrogen and carbon, respectively. When the A_{600} of cell growth reached about 0.6, protein expression was induced by adding isopropyl β-D-1-thiogalactopyranoside (IPTG) at a final concentration of 1 mM. To produce the protein as a zinc-bound form, 1 mM $ZnSO_4$ was added simultaneously. After 6 hrs incubation, cells were harvested by centrifugation and resuspended in lysis buffer (25 mM Tris-HCl, 1 mM DTT, 1 mM $ZnSO_4$, pH 7.5). The cells were disrupted by sonication on ice and Hsp33 was purified from the supernatant, initially via sequential applications of two anion exchange chromatography steps on a HiTap Q-Sepharose FF and a HiTrap Q HP column (GE Healthcare). Subsequently, the gel-permeation chromatography on a HiLoad 16/60 Superdex 75 column (GE Healthcare) was employed as the final purification step. For oxidation, the purified solution of reduced, zinc-bound Hsp33, was buffer-exchanged using PD-10 column in oxidation buffer (40 mM HEPES-KOH, 5 mM H_2O_2, pH 7.5).[7,8] Oxidation of 50 μM Hsp33 was performed by incubating the solution at 43°C for 3 hrs. The Oxidized Hsp33 solution was concentrated and applied onto a HiLoad 16/60 Superdex 75 column, which was pre-equilibrated with a 20 mM Tris-HCl, 50 mM NaCl, at pH 6.5. The fractions of half-oxidized Hsp33 were selectively pooled[4,5] and concentrated to 0.6 mM for NMR measurements. Protein concentration was estimated using the molar absorptivity (29,285 $M^{-1}cm^{-1}$ at 280 nm) predicted from the amino acid sequence.

NMR measurements and assignments - Conventional 2D-[^{1}H, ^{15}N]TROSY and two kinds of triple resonance spectra (HNCACB and HNCO) were acquired at 313 K on a Bruker Biospin Avance 900 spectrometer equipped with a cryoprobe. All NMR spectra were processed using the NMRPipe software and analyzed with the NMRViewJ program. Chemical shift perturbations were evaluated as their weighted average variations (Δ_{AVE}), using the $^1H^N$ ($\Delta\delta_H$) and $^{15}N^\alpha$ ($\Delta\delta_N$) chemical shifts: $\Delta_{AVE} = [(\Delta\delta^2_H + \Delta\delta^2_N/25)/2]^{1/2}$.[9]

Results and Discussion

It has been previously known that the interesting molecular chaperone, Hsp33 entails massive conformational rearrangements involving a significant unfolding for its functional activation. Furthermore, it has been suggested that Hsp33 can adopt many different conformations depending on its redox and functional status. Particularly, even in the oxidized state, at least four different species could be distinguished in our previous study: half-oxidized monomeric form and fully-oxidized monomeric, dimeric, and oligomeric forms.[4] Thus, in the present work, we could successfully isolate the half-oxidized form and measured its NMR spectra at 313 K and at pH 6.5, under which condition the reduced Hsp33 conformation was investigated previously.[5] The 2D-[^{1}H, ^{15}N]TROSY spectrum of the half-oxidized Hsp33 is characterized by a significant collapse in the middle of the spectrum, with a still remaining abundance of resolved peaks (Fig. 1). For sequence-specific assignments, we first verified peak clusters of individual resonances by collecting related peaks in the triple resonance spectra. Each peak cluster contained the intra- and inter-residue chemical shift information about the carbon atoms: $^{13}C^\alpha$(i), $^{13}C^\alpha$(i-1), $^{13}C^\beta$(i) and $^{13}C^\beta$(i-1) from HNCACB spectrum and ^{13}CO(i-1) from HNCO spectrum. However, unfortunately, the significant peak overlapping in the collapsed region prevented us from distinguishing the corresponding resonances in the triple resonance spectra. As Hsp33 consists of 294 amino acids including the N-terminal residue and 14 prolines, the theoretical number of backbone amide resonances that can be observed is 279. We could unambiguously isolate just 170 (61%) of peak clusters. In addition, 33 of them, of which majority was from the collapsed region, could not be assigned due to the lack of an enough sequential connectivity. Consequently, the carbon chemical shift information from the HNCACB and HNCO spectra was not sufficient for the sequence-specific assignments to whole region of the protein. Nonetheless, we could assign almost all of the resolved peaks, by linking the peak clusters according to the (i-1)-(i) carbon

connectivities. The previously assigned chemical shift data for reduced Hsp33 were also used to find corresponding peaks in the half-oxidized Hsp33 spectra. Finally, the assigned chemical shifts are summarized in Table 1. The assignments extent, including $^{1}H^{N}$, ^{15}N, $^{13}C^{\alpha}$, $^{13}C^{\beta}$, and ^{13}CO atoms, was just around 50% (Fig. 1 and Table 1). However, inspection of the non-assigned regions and the chemical shift comparison between reduced and half-oxidized states can provide useful information about the oxidation-induced conformational change.

Table 1. Assigned chemical shifts (ppm) of $^{1}H^{N}$, ^{15}N, $^{13}C^{\alpha}$, $^{13}C^{\beta}$ and ^{13}CO atoms of half-oxidized Hsp33 at 313K and pH 6.5. (NA, not available; ND, not detected)

a.a.	$^{1}H^{N}$	^{15}N	$^{13}C^{\alpha}$	$^{13}C^{\beta}$	^{13}CO
I2	ND	ND	60.7	38.1	175.72
M3	8.5	125.6	52.3	32.0	173.50
L9	9.4	125.1	53.6	44.0	ND
Y12	ND	ND	55.3	39.7	174.01
L13	9.1	121.5	54.2	45.8	ND
V19	ND	ND	60.0	35.8	173.92
R20	9.5	125.4	53.7	32.9	174.06
G21	8.7	107.7	43.2	G	ND
E22	ND	ND	53.7	34.1	174.18
L23	9.2	124.2	54.3	46.0	174.51
V24	9.8	126.8	58.9	36.6	173.06
T25	8.0	116.7	61.0	70.3	173.79
V26	8.4	110.8	59.2	32.9	ND
L34	ND	ND	57.0	41.1	178.31
E35	7.5	120.1	57.2	29.2	ND
N36	ND	ND	55.0	37.4	174.25
H37	7.7	114.8	54.9	30.2	ND
P42	NA	NA	65.6	31.8	179.19
V43	7.1	115.1	64.3	31.4	176.96
K44	7.8	119.5	60.4	31.4	178.91
N45	8.0	116.0	55.9	37.4	177.07
V46	7.4	119.7	65.7	30.6	ND
A48	ND	ND	55.5	19.2	179.15
E49	8.1	117.1	60.0	29.4	179.05
L50	8.9	119.5	57.0	41.9	180.32
L51	8.8	125.3	58.4	40.9	ND
V52	ND	ND	66.3	30.8	177.95
A53	8.7	118.9	55.3	17.9	179.11
T54	8.6	114.6	68.3	67.1	181.83
L57	8.9	121.9	58.4	40.9	ND
T58	ND	ND	ND	68.6	175.38
A59	7.0	118.5	52.8	19.3	177.92
T60	7.7	110.0	62.7	69.9	174.72
L61	7.5	123.0	54.3	43.1	ND
K62	ND	ND	55.3	31.7	174.86
F63	7.6	120.5	55.2	40.2	ND
D64	ND	ND	53.0	42.0	175.48
G65	8.3	111.5	45.4	G	ND
I67	ND	ND	58.3	40.8	173.10
T68	9.1	123.8	61.3	70.8	173.27
V69	9.1	128.4	61.3	32.1	173.86
Q70	9.0	124.9	53.0	32.7	173.80
L71	9.5	126.3	53.2	43.5	175.11
Q72	8.7	122.5	53.2	32.1	174.04
G73	8.1	108.3	46.1	G	172.84
D74	7.8	118.0	52.3	40.4	177.75
G75	8.0	109.7	43.5	G	ND
M77	ND	ND	53.4	33.4	172.40
N78	7.4	118.2	53.8	38.3	ND
L79	ND	ND	54.3	45.4	175.06
A80	8.9	127.3	52.0	20.7	174.67
V81	9.1	121.4	59.3	35.0	173.41
I82	8.6	124.6	57.0	36.5	ND
N85	ND	ND	52.0	40.6	176.13
N86	8.7	113.4	55.7	37.5	174.83
N87	7.9	117.9	53.2	38.3	ND
V93	ND	ND	61.0	35.0	171.11
A94	7.6	123.4	50.3	22.4	175.22
R95	9.1	121.3	55.0	32.4	ND
V96	ND	ND	60.0	34.0	176.02
Q97	9.5	125.4	54.3	29.8	174.93
G98	7.9	110.3	44.0	G	ND
E99	ND	ND	56.0	29.8	176.09
I100	8.6	124.6	56.0	37.7	ND
P101	NA	NA	62.0	31.7	176.65
E102	8.6	120.7	57.8	29.3	177.13
N103	8.7	116.1	52.8	37.5	174.97
A104	7.3	120.6	52.9	19.7	176.39
D105	7.9	121.2	51.4	41.2	ND
L106	ND	ND	59.0	41.3	178.32
K107	8.3	116.0	58.9	30.7	180.05
T108	8.1	117.7	65.6	67.5	ND
L109	ND	ND	57.7	42.2	176.41
V110	8.1	112.5	61.6	33.0	177.90
G111	7.9	110.3	45.3	G	174.93
N112	9.2	125.9	52.6	37.8	175.64
G113	8.1	111.7	45.5	G	172.52
Y114	8.7	116.1	56.6	41.0	173.58
V115	9.1	120.0	59.9	32.7	174.75
V116	9.3	126.4	60.3	33.2	176.00
I117	9.2	130.9	60.3	39.5	175.13
T118	9.2	123.6	61.0	69.6	174.18
I119	9.4	130.1	60.0	39.2	174.98
T120	9.1	124.4	58.4	ND	ND
P121	NA	NA	61.0	32.0	176.85
S122	9.1	118.3	60.4	62.7	ND
E123	ND	ND	55.5	31.0	175.22
G124	8.2	110.6	43.7	G	ND
R126	ND	ND	56.1	30.8	175.70
Y127	8.9	124.1	56.2	40.4	ND
Q128	ND	ND	54.0	33.1	174.26
G129	9.1	113.9	44.0	G	ND
V130	ND	ND	60.2	34.6	175.60
V131	9.3	126.2	60.3	34.3	175.07
G132	8.8	113.0	44.8	G	ND
E134	ND	ND	56.5	29.8	177.35
G135	7.9	108.6	44.1	G	173.09
D136	8.5	116.1	55.4	41.4	176.56
T137	7.5	106.4	58.2	71.9	175.00
L138	9.6	125.4	58.0	40.4	179.19
A139	9.2	120.4	55.6	18.0	178.78
A140	7.8	118.6	54.6	18.4	181.33
C141	7.9	117.3	61.9	26.6	179.20
E143	8.8	121.3	60.5	28.6	179.62
D144	7.8	120.1	57.4	40.8	ND
M147	ND	ND	58.0	30.1	178.74
R148	8.6	118.4	58.3	30.1	178.27

S149	8.3	113.4	60.1	63.0	ND
E150	ND	ND	55.5	29.9	175.65
Q151	7.6	114.4	56.7	25.7	ND
P153	NA	NA	64.2	30.3	174.84
T154	7.9	120.7	62.0	72.5	173.31
R155	9.4	124.5	51.8	33.0	174.18
L156	9.7	123.7	53.7	45.4	174.55
F157	9.0	120.8	55.6	39.3	174.52
I158	9.1	123.9	61.3	39.1	175.94
R159	9.2	127.2	52.7	32.1	174.42
T160	8.4	112.3	59.1	70.5	173.37
G161	8.2	108.5	45.6	G	170.85
D162	8.3	122.1	53.1	43.3	175.60
V163	9.0	121.8	61.4	33.3	176.48
D164	9.4	128.9	55.0	39.6	175.94
G165	8.7	103.8	45.1	G	174.43
K166	7.8	122.1	52.8	33.0	ND
P167	NA	NA	63.4	31.9	175.16
A168	8.3	123.0	50.5	23.5	ND
A169	ND	ND	51.8	23.1	174.96
G170	9.0	107.2	46.0	G	170.57
G171	9.5	106.6	46.6	G	173.62
L173	9.1	123.8	53.4	47.1	175.28
L174	9.2	125.3	53.4	47.3	176.18
Q175	9.4	122.6	55.0	34.6	174.42
V176	7.4	125.8	63.0	32.4	177.55
Q180	8.1	117.5	55.2	ND	175.58
N181	8.5	117.8	53.0	38.1	170.89
M172	9.4	116.9	54.0	38.0	174.69
A182	8.2	123.8	52.2	19.5	177.97
Q183	9.1	121.6	54.7	28.2	177.39
D185	8.8	117.4	ND	ND	177.67
F187	7.8	121.6	61.6	38.3	176.69
D188	8.9	118.9	57.0	39.6	ND
L190	ND	ND	57.1	40.8	180.78
A191	8.8	126.6	55.6	17.5	178.82
T192	8.3	116.9	66.1	68.0	ND
L193	ND	ND	56.3	41.5	179.30
T194	7.6	116.1	65.7	68.3	173.76
E195	7.5	117.6	57.4	29.4	176.62
T196	7.0	106.3	62.3	69.2	175.66
I197	7.5	123.4	58.9	37.9	174.72
K198	8.7	128.5	54.4	33.0	178.46
T199	9.2	123.1	61.1	68.1	174.99
E200	9.6	117.3	59.5	28.3	178.99
E201	7.0	118.9	58.5	29.5	176.63
L202	7.6	117.4	57.2	41.4	176.90
L203	7.7	108.8	55.1	41.1	178.47
T204	7.4	105.5	61.9	70.8	174.49
L205	7.7	123.6	52.2	41.1	ND
P206	NA	NA	61.8	31.7	178.44
A207	8.7	126.1	55.1	17.4	178.77
N208	8.6	111.5	56.3	36.7	177.53
E209	7.3	120.6	58.3	29.0	178.82
V210	7.8	121.6	66.6	30.9	ND
R213	ND	ND	59.0	29.2	178.73
L214	7.7	115.8	56.3	41.2	ND
V220	ND	ND	60.0	34.3	174.87
T221	8.9	125.4	61.5	ND	173.09
V222	8.6	126.8	61.1	32.5	176.14
Y223	8.4	126.2	55.7	38.0	174.82
D224	8.6	120.3	53.5	39.5	ND
P225	NA	NA	62.2	31.7	176.54
Q226	8.7	120.0	53.8	31.8	175.00
D227	8.8	126.4	55.5	40.8	ND
V228	ND	ND	ND	33.8	175.18
E229	8.8	123.3	54.3	33.8	ND
A289	ND	ND	52.0	19.0	177.36
D290	8.2	121.2	51.9	40.7	ND
Q292	ND	ND	55.4	28.9	176.01
V293	8.0	121.3	61.9	32.0	175.29
H294	8.0	127.5	56.5	30.0	ND

As addressed above, the missing assignments are mostly attributed to the severe peak overlaps with strong peak intensities in the middle of the spectra. These characteristics indicated that the resonances in the collapsed spectral region originated probably from flexible, unfolded regions in the protein structure. Fig. 2(a) shows that those missing assignments are largely mapped onto the C-terminal redox-switch domain, which is well-folded in the reduced state. Many of the other regions with the missing assignments in the half-oxidized state were consistent with the regions that didn't show NMR signals even in reduced state, probably due to a certain conformational exchange at an intermediate rate in NMR time scale.[5] Thus, the peculiar dynamic properties of reduced Hsp33 seem to be retained in the half-oxidized state. Meanwhile, the assigned chemical shifts of the half-oxidized form are generally in good agreement with those assigned previously in the reduced Hsp33. All those results support the previously established model for the half-oxidized Hsp33; *i.e.*, the half oxidation results in the partial unfolding that is localized mainly in the C-terminal redox-switch domain. In addition, this conformation is not likely to bind the unfolding intermediates of client proteins, as no hydrophobic regions are expected to be exposed to bind substrates upon the conformational change. Thus, as previously suggested by Ilbert *et al.*,[10] the half-oxidized conformation would be closer to an inactive form, rather than active or partially active states.

However, it should be noted that some of the assignment-missing regions in the N-terminal domain of the half-oxidized form were those assigned in the reduced Hsp33. In addition, some of the assigned chemical shifts in half-oxidized state were significantly different from those assigned in reduced state. Fig. 3 shows chemical shift perturbations

(CSPs) of the assigned resonances and the relatively higher values of Δ_{AVE} were mapped on the structure in Fig. 2(b). The residues with Δ_{AVE} over 0.04 ppm were L9, H37, E49, L57, T68, V69, Q70, N78, V81, N86, A94, G113, I117, G129, S149, R155, Q175 and V176 from the N-terminal core domain, Q180 from the middle linker domain and E229 from the extended linker stretch. These results suggest that some regions out of the C-terminal redox-switch domain would undergo, albeit slightly and sporadically, a conformational change upon the half oxidation. It is also noteworthy that the unusual dynamics observed in the reduced state would be retained in the half-oxidized state. In addition, interestingly, we observed that several amide $^{1}H^{N}$-^{15}N resonances (A53, S149, R155, L156, and three non-assigned resonances) of the half-oxidized Hsp33 split into two peaks with nearly identical $^{13}C^{\alpha}$, $^{13}C^{\beta}$, and ^{13}CO chemical shifts. The splitting peaks are presumably indicative of a certain chemical exchange at a slow rate. One of the divided $^{1}H^{N}$-^{15}N chemical shifts was consistent with that in the reduced Hsp33. Thus, these residues are likely to possess an altered dynamic property, compared to the reduced form.

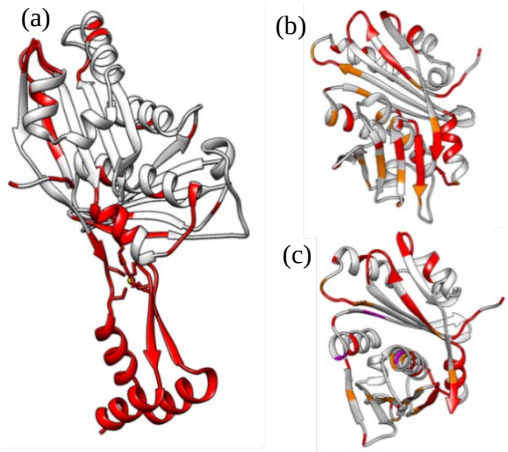

Figure 2. The semi-empirical structure model of the reduced, inacive Hsp33 monomer.[5] (b) and (c) show only the N-terminal core domain. Assignment results for the half-oxidized Hsp33 are depicted in different colors: red, assignment-missing residues (a-c); orange, residues with relatively significant chemical shift perturbations (b and c); magenta, resonance-splitting residues. The figures were generated, using the UCSF Chimera program.[11]

They are located in the core domain (in α2, α4, and β8 elements), as mapped onto the structure in Fig. 2(c).

Collectively, all these results suggest that certain additional changes in conformation and/or dynamics occurred in the N-terminal core domain, even though they are relatively trifling compared to the dramatic unfolding of the C-terminal redox-switch domain. As mentioned above, most of the resolved peaks were assigned in the half-oxidized Hsp33 spectrum. Therefore, we postulate that the additional change would also resemble an unfolding, which can result in the resonance shift to the collapsed region, or increased dynamic perturbation, which can result in disappearance of the signals due to severe line broadening. Particularly, it is suggested that dynamic regions in inactive state are structural determinants regulating the activation process of Hsp33.[5] Likewise,

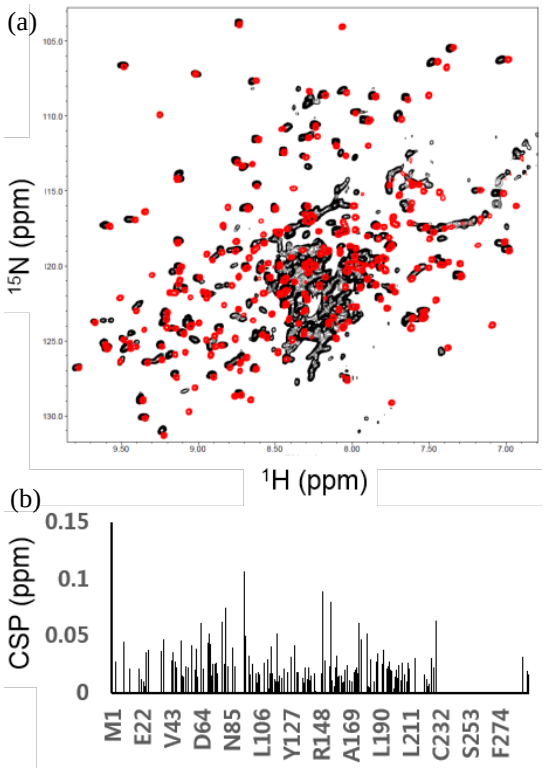

Figure 3. (a) Superimposition of the [^{1}H, ^{15}N]TROSY spectra of reduced Hsp33 (red) and half-oxidized Hsp33 (black). (b) Backbone amide chemical shift perturbations between reduced Hsp33 and half-oxidized Hsp33.

the increased dynamics in the half-oxidized form would be also responsible for lowering energy barrier for converting to the fully active conformation. In this respect, we speculate that the half-oxidized conformation would be more labile to heat and/or oxidative stressors to facilitate the final activation process; *i.e.*, it is a stable, intermediate state between the reduced, inactive form and the fully oxidized, active form.

Acknowledgements

This paper was written as part of Konkuk University's research support program for its faculty on sabbatical leave in 2014. This research was supported by Basic Science Research Program through the National Research Foundation of Korea (NRF) funded by the Ministry of Education, Science and Technology (No. 2010-0006022 and in part 2013R1A1A2007774). The NMR experiments in particular were supported by a grant from the High-Field NMR Research Program of the Korea Basic Science Institute.

References

1. U. Jakob, W. Muse, M. Eser, and J.C.A. Bardwell, *Cell* **96**, 341 (1999)
2. P.C.F. Graf and U. Jakob, *Cell. Mol. Life. Sci.* **59**, 1624 (2002)
3. J. Winter, M. Ilbert, P.C. Graf, D. Ozecelik, and U. Jakob, *Cell* **135**, 691 (2008)
4. Y.-S. Lee, K.-S. Ryu, S.-J. Kim, H.-S. Ko, D.-W. Sim, Y.H. Jeon, E.-H. Kim, W.-S. Choi, and H.-S. Won, *FEBS Lett.* **586**, 411 (2012)
5. Y.-S. Lee, J. Lee, K.-S. Ryu, Y. Lee, T.-G. Jung, J.-H. Jang, D.-W. Sim, E.-H. Kim, M.-D. Seo, K.W. Lee, and H.-S. Won, *J. Mol. Biol.* **427**, 3850 (2015)
6. Y.-S. Lee, H.-S. Ko, K.-S. Ryu, Y.-H. Jeon, and H.-S. Won, *J. Kor. Magn. Reson. Soc*. **14**, 117 (2010)
7. M. Ilbert, P.C.F. Graf, and U. Jakob, *Antitoxid. Redox. Signal* **8**, 835 (2006)
8. Y.-S. Lee, K.-S. Ryu, Y. Lee, S. Kim, K. W. Lee, and H.-S. Won, *J. Kor. Magn. Reson. Soc*. **15**, 137 (2011)
9. S. Grzesiek, S.J. Stahl, P.T. Wingfield, and A. Bax, *Biochemistry* **35**, 10256 (1996)
10. M. Ilbert, J. Horst, S. Ahrens, J. Winter, P.C.F. Graf, H. Lilie, and U. Jakob, *Nat. Struct. Mol. Biol.* **14**, 556 (2007)
11. E.F. Pettersen, T.D. Goddard, C.C. Huang, G.S. Couch, D.M. Greenblatt, E.C. Meng, and T.E. Ferrin, *J. Comput. Chem*. **25**, 1605 (2004)